Available online at www.sciencedirect.com
SCIENCE DIRECT®
Biochemical and Biophysical Research Communications 300 (2003) 87–92
BBRC
www.elsevier.com/locate/ybbrc

Influence of TFIIIA-type linker at the N- or C-terminal of nine-zinc finger protein on DNA-binding site☆

Wataru Nomura, Makoto Nagaoka, Yasuhisa Shiraishi, and Yukio Sugiura*

Institute for Chemical Research, Kyoto University, Uji, Kyoto 611-0011, Japan

Received 11 November 2002

Abstract

The central three-zinc finger connection of the native nine-zinc finger protein transcription factor IIIA (TFIIIA) is composed of unique linker sequences, –NIKICV–, –TQQLP–, –AG–, and –QDL–. New artificial nine-zinc finger proteins, Sp1ZF9TC and Sp1ZF9TN, which use the TFIIIA-type linker for their C- and N-terminal three-zinc finger connections have been created. To investigate the influence of TFIIIA-type linker sequences by their different locations in the proteins, gel mobility shift assays (GMSA), DNase I footprinting assays, methylation interference analyses, and hydroxyl radical footprinting assays were performed. The GMSA revealed similar DNA-binding affinities of these two proteins. The footprinting analyses indicated that the two zinc finger proteins recognize the same part of GCII or GCIII DNA. Moreover, the specific base contacts were observed in the same sites of the substrate DNA. In the present proteins, Sp1ZF9TC and Sp1ZF9TN, the four zinc fingers (fingers 1–4 or 5–9) situated in the site opposite to the TFIIIA-type linker position participate in their DNA bindings. The position of the TFIIIA-type linker is important in DNA recognition by multi-zinc finger proteins.

Keywords: Zinc finger; Linker sequence; Krüppel-type linker; Sp1; TFIIIA; Nine-finger protein

The Cys_2His_2-type zinc finger motif consists of tandem repeats of zinc-binding mini-domains connected by short linker sequences. Each mini-domain is folded as a $\beta\beta\alpha$ conformation by the coordination of a zinc ion with the invariant two cysteines and two histidines [1]. In natural zinc finger proteins, the short linker sequence, Thr–Gly–Glu–Lys–Pro, is the most typical linker sequence (*Krüppel-type* linker) between each finger domain [2,3]. Zinc finger proteins recognize a specific DNA sequence by locating its α-helix in the major groove of DNA [4]. The utilization of zinc finger proteins for DNA sequence recognition has been investigated from the recognition helix experiments of zinc finger proteins by several design- [5,6] and phage-display-based [7–11] mutational analyses. Some natural zinc finger proteins control their DNA- and/or RNA-binding mode by the unique linker sequences [12,13]. The transcription factor TFIIIA derived from *Xenopus oocyte* is one of the most famous nine-zinc finger proteins [14,15]. As revealed by an X-ray crystallographic study of the TFIIIA-5S rRNA gene complex, the characteristic DNA-binding mode of the TFIIIA zinc finger protein is based on the unique linker sequences that connect the central five-zinc finger domains [16]. Recently, we designed and created a new artificial nine-zinc finger protein, Sp1ZF9T, which contains the TFIIIA-type linker sequences in the central part of the nine-zinc finger protein, Sp1ZF9 [17,18]. Sp1ZF9T showed a DNA-binding mode different from that of Sp1ZF9 containing only the (*Krüppel-type* linker), and this result strongly indicated that the linker sequences have a significant effect on the DNA-binding mode in a multi-zinc finger protein. By modification of the linker sequences [19] and adjustment of the linker length [20,21], several efforts to improve the

☆ This study was supported in part by a Grant-in-Aid for the COE Project "Element Science" (12CE2005) and Scientific Research (12793008, 13557210, and 14370755) from the Ministry of Education, Culture, Sports, Science and Technology, Japan. W.N. is a research fellow of the Japan Society for the Promotion of Science.

* Corresponding author. Fax: +81-774-32-3038.
E-mail address: sugiura@scl.kyoto-u.ac.jp (Y. Sugiura).

0006-291X/02/$ - see front matter © 2002 Elsevier Science (USA). All rights reserved.
PII: S0006-291X(02)02792-4

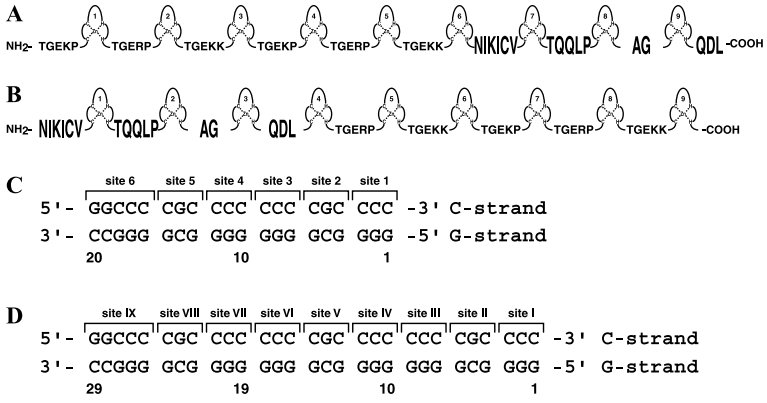

Fig. 1. Schematic representations of the new artificial nine-zinc finger proteins Sp1ZF9TC (A) and Sp1ZF9TN (B), and their substrate DNA sequences, GCII DNA (C) and GCIII DNA (D). Amino acid residues of the linker sequences are indicated by one-letter abbreviations. GCII DNA consists of sites 1–6 and GCIII sites I–IX. The numbers indicate the position of the bases.

DNA-binding affinity have also been performed. However, it is unknown whether the position of the linker sequences in multi-zinc finger protein has any effect on DNA bindings. We newly created the artificial nine-zinc finger proteins, Sp1ZF9TC and Sp1ZF9TN, which contain the TFIIIA-type linker sequence in the C- and N-terminal sites (see Fig. 1). Herein, our artificial nine-zinc finger proteins use only the four-finger domains for DNA recognition and also recognize the same site of substrate DNA. In the control of the numbers of the zinc finger domains utilized for DNA recognition and the recognition specificity for the desired sequences, the present results would provide useful information for the design and engineering of artificial multi-zinc finger proteins.

Materials and methods

Chemicals. T4 polynucleotide kinase was obtained from New England Biolabs. The labeled compound [γ-^{32}P]ATP was supplied by DuPont. The synthetic oligonucleotides for mutagenesis were purchased from Amersham Pharmacia Biotech. All other chemicals used were of commercial reagent grade.

Construction of genes and protein expression. To prepare the gene for Sp1ZF9TN and Sp1ZF9TC, the gene for Sp1ZF9T constructed previously was used [18]. For the gene of Sp1ZF9TN, the sequence for the region of fingers 1–6 for Sp1ZF6 was amplified by a polymerase chain reaction (PCR) with appropriate primers for fingers 4–9 of Sp1ZF9TN. On the other hand, the region of fingers 4–6 of Sp1ZF9T was used for fingers 1–3 of Sp1ZF9TN. These two fragments were digested by *Ava*II restriction enzyme and ligated. The resultant fragment was inserted into pEV3b as a *Bam*HI/*Eco*RI fragment. For the gene of Sp1ZF9TC, the sequence for the region of fingers 1–6 of Sp1ZF9T was amplified by a PCR with appropriate primers for fingers 4–9 of Sp1ZF9TC and then inserted into pEV3b. We renamed this plasmid pEVStyIdel. The gene coding the region of fingers 1–3 for Sp1ZF9TC was cut out by StyI from pUCSp1OL, which was constructed previously [18]. This fragment was inserted into pEVStyIdel. These proteins were expressed in an *Escherichia coli* strain BL21(DE3) pLysS and purified according to the previous method [5]. The purified peptides, Sp1ZF9TN and Sp1ZF9TC, were dialyzed as previously described [17] and used in the experiments.

Gel mobility shift assays. Gel mobility shift assays were carried out under the following conditions. As the substrate DNAs, GCIII DNA and GCII DNA were utilized. Each reaction mixture contained 10 mM Tris buffer (pH 8.0), 100 ng/μl poly(dI–dC), 5% glycerol, the 5′-end labeled *Sac*I–*Kpn*I fragment of substrate DNA (~100 pM), and 0–1000 nM protein. After incubation at 20 °C for 0.5 h, the samples were run on a 10% polyacrylamide gel with 1× TB buffer at 20 °C. The bands were visualized by autoradiography and analyzed using ImageQuant software (Amersham Bioscience).

DNase I footprinting analyses. DNase I footprinting experiments were performed according to the method of Brenowitz et al. [22]. The reaction mixture contained 10 mM Tris buffer (pH 8.0), 50 mM NaCl, 5 mM $CaCl_2$, 20 ng/μl sonicated calf thymus DNA, the 5′-end labeled *Sac*I–*Kpn*I fragment of substrate DNA (approximately 20 Kcpm), and 0–500 nM protein. After incubation at 20 °C for 30 min, the samples were digested with DNase I (70 mU) at 20 °C for 2 min. The reaction was stopped by the addition of 30 μl DNase I stop solution (0.1 M EDTA and 0.6 M sodium acetate) and 50 μl phenol/chloroform. After ethanol precipitation, the cleavage products were analyzed on a 10% polyacrylamide/7 M urea sequencing gel. The bands were visualized by autoradiography and quantified with ImageQuant software.

Methylation interference analyses. Methylation interference analyses were carried out as described previously [23]. The reaction mixture contained 10 mM Tris buffer (pH 8.0), 100 ng/μl poly(dI–dC), 5% glycerol, the 5′-end labeled methylated *Sac*I–*Kpn*I fragment of substrate DNAs (approximately 20 Kcpm), and 500 nM protein. To examine both the strong and weak base contacts, we selected the experimental conditions in which the peptide/DNA molar ratio in the binding reaction was about 10–20% bound. The electrophoresis bands were visualized by autoradiography and analyzed using ImageQuant software (Amersham Bioscience).

Hydroxyl radical footprinting analyses. Hydroxyl radical footprinting experiments were carried out according to the method reported by Tullius et al. [24]. The binding reaction mixture contained 20 ng/μl sonicated calf thymus DNA, the 5′-end labeled methylated *Sac*I–*Kpn*I fragment of substrate DNA (approximately 20 Kcpm), and 250 nM protein. After incubation at 20 °C for 30 min, the samples were cleaved by additions of 100 mM ferrous ammonium sulfate, 200 mM EDTA, and 0.003% hydrogen peroxide at 20 °C for 1 min. The reaction was quenched by adding 20 μl hydroxyl radical stop solution (0.135 M thiourea, 0.135 M EDTA, and 0.6 M sodium acetate). After phenol extraction and ethanol precipitation, the cleavage products were analyzed on a 15% polyacrylamide/7 M urea sequencing gel. The bands were visualized by autoradiography and quantified with ImageQuant software.

Results and discussion

Comparison of DNA-binding affinity between Sp1ZF9TC and Sp1ZF9TN

The DNA bindings of the new artificial nine-zinc finger proteins, Sp1ZF9TC and Sp1ZF9TN, were determined by gel mobility shift assays. Fig. 2 shows the DNA-binding properties of Sp1ZF9TC and Sp1ZF9TN. The two shifted bands, namely B-1 and B-2, were detected for binding to GCIII DNA (Figs. 1D, 2C, and D). These bands were similarly observed in the previous case of Sp1ZF9T [18]. As shown in the previous study, B-1 indicates the long-lived DNA–protein

Fig. 2. Gel mobility shift assays for Sp1ZF9TC and Sp1ZF9TN bindings to GCII and GCIII DNAs. The panels (A–D) depict the results for bindings of Sp1ZF9TC–GCII DNA (A), Sp1ZF9TN–GCII DNA (B), Sp1ZF9TC–GCIII DNA (C), and Sp1ZF9TN–GCIII DNA (D). The lanes 1–9 in each panel present 0, 5, 10, 20, 50, 100, 200, 500, and 1000 nM protein, respectively. F, B-1, and B-2 show free DNA, long-lived protein–DNA complex species, and short-lived species, respectively.

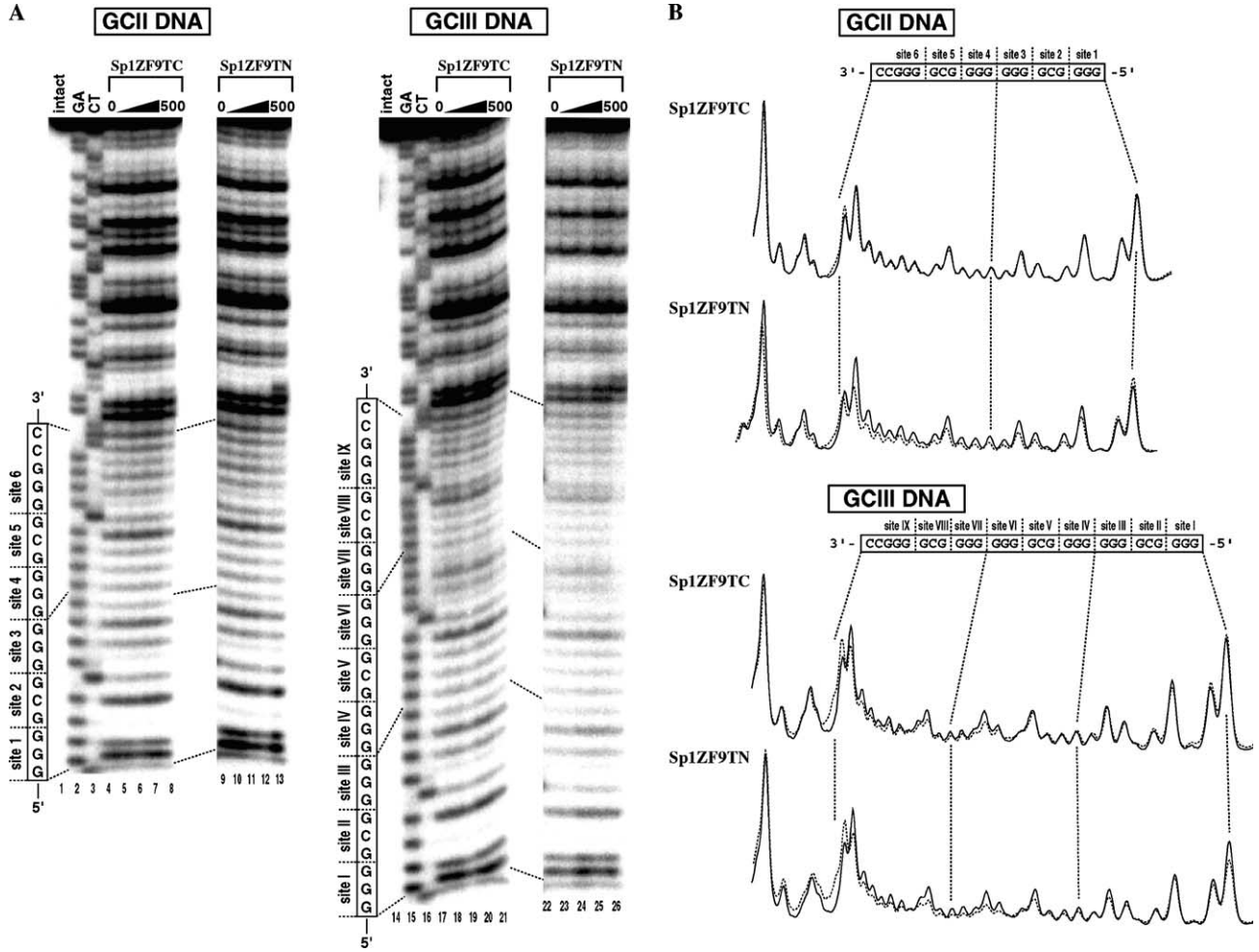

Fig. 3. DNase I footprinting analyses for Sp1ZF9TC and Sp1ZF9TN binding to GCII and GCIII DNAs. (A) Autoradiograms of electrophoresis gels. The left (lanes 1–13) and right (lanes 14–26) panels show the results for GCII and GCIII DNAs, respectively. Lanes 1 and 14, intact DNA; lanes 2 and 15, G + A (Maxam–Gilbert reaction products); lanes 3 and 16, C + T (Maxam–Gilbert reaction products); lanes 4–8, 9–13, 17–21, and 22–26, protein-bound DNA samples. The protein concentrations for each sample are 0, 50, 125, 250, and 500 nM, respectively. (B) Densitometric analyses of the autoradiograms. The results with 500 nM protein and without protein are represented by dotted and solid lines, respectively.

complex and B-2 the short-lived complex. This was confirmed by the same experiments after 72 h of the binding reaction (data not shown). The binding affinities for GCIII DNA of the two proteins were almost the same. GCII DNA was also used as the substrate for the Sp1ZF9TC and Sp1ZF9TN, because these two proteins contain the part to which six-zinc finger domains are connected by the canonical linker sequences (Fig. 1C). In the binding experiment for GCII DNA, our zinc finger proteins Sp1ZF9TC and Sp1ZF9TN showed the formation of a stable 1:1 complex with the GCII DNA (Figs. 2A and B).

Differences in DNA-binding mode of nine-zinc finger proteins

To estimate the detailed DNA-binding mode of the present proteins, DNase I footprinting analyses were performed. As clearly shown in Fig. 3, the two kinds of proteins, Sp1ZF9TC and Sp1ZF9TN, bind to the 3′-portion of the GCII and GCIII DNA. However, there is a difference in the enhancement of the DNA digestion by DNase I nuclease that indicates a DNA conformational change caused by the protein binding. In the DNA binding of Sp1ZF9TN, the stronger enhancement of DNA digestion was clearly observed at the 3′-external region of the target GC-rich DNA sequences (Fig. 3A, lanes 13 and 26). Probably, this difference in enhancement suggests the different location of proteins on the substrate DNAs due to the different positions of TFIIIA-type linker sequences.

Fig. 4 shows the results of the methylation interference analyses for bindings to the GCII and GC III DNAs of the proteins. To confirm the DNA base contacts for the G- and C-strand (data not shown), experiments were performed for both of the DNA strands. The two proteins form the same specific DNA base contacts with substrate DNA at sites 3–6 for GCII DNA and sites VI–IX for GCIII DNA (Fig. 4B). These results indicate that our nine-zinc finger proteins, Sp1ZF9TC and Sp1ZF9TN, use only four-zinc finger domains to recognize the specific DNA base contacts. In addition, the results of the bindings to the C-strand also support the fact that the DNA base contacts of these zinc finger

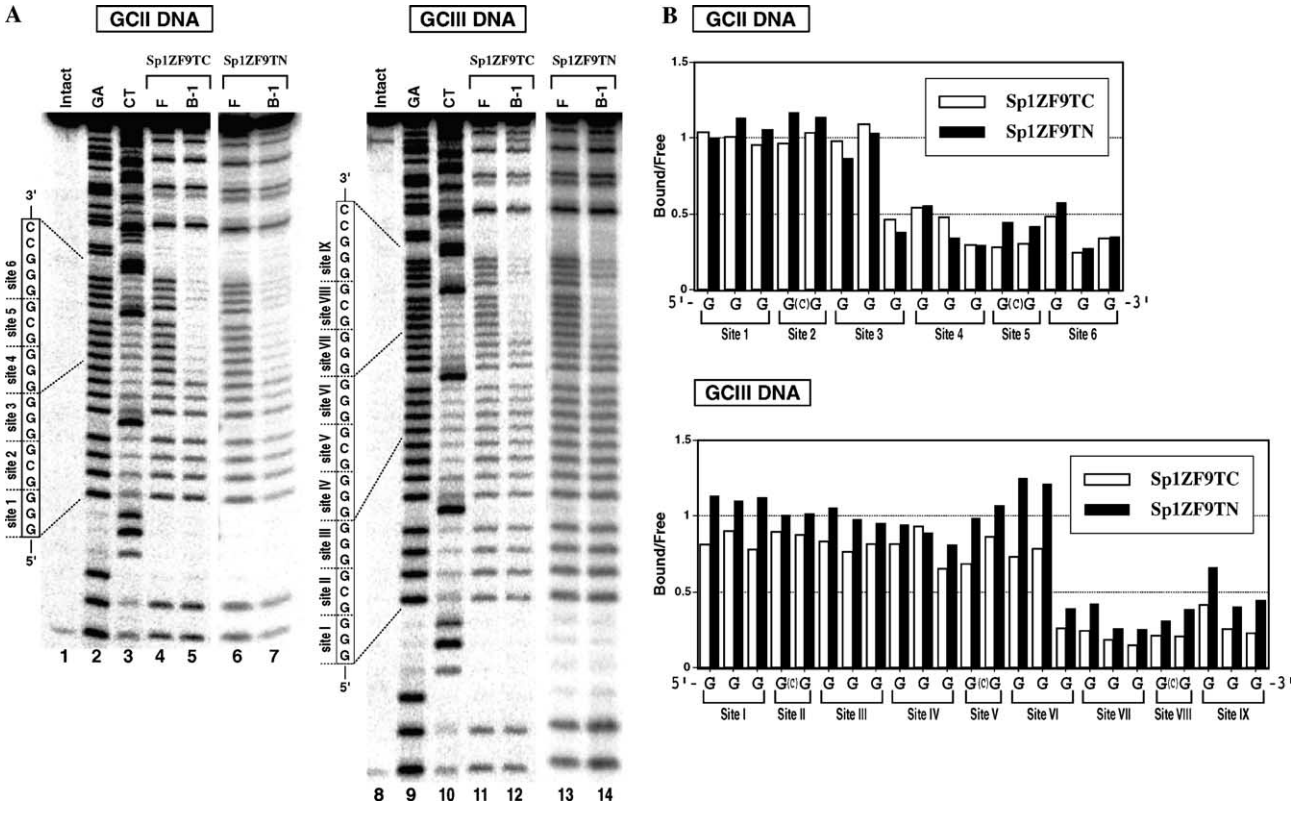

Fig. 4. Methylation interference analyses for Sp1ZF9TC and Sp1ZF9TN bindings to GCII and GCIII DNAs. The reaction mixture was incubated at 20 °C for 30 min. (A) Autoradiograms of electrophoresis gels. The left (lanes 1–7) and right (lanes 8–16) panels show the results for the GCII and GCIII DNAs, respectively. Lanes 1 and 8, intact DNA; lanes 2 and 9, G + A (Maxam–Gilbert reaction products); lanes 3 and 10, C + T (Maxam–Gilbert reaction products); lanes 4, 6, 11, and 13, protein-free DNA; lanes 5 and 7, protein–GCII DNA complexes; and lanes 12 and 14, B-1 complex species, respectively. (B) Histograms showing the extent of methylation interference by Sp1ZF9TC and Sp1ZF9TN bindings to GCII and GCIII DNAs. The autoradiograms of the gels were scanned with a densitometer, and the extent of interference was calculated as the ratio of the cutting probabilities for the two bands (bound/free).

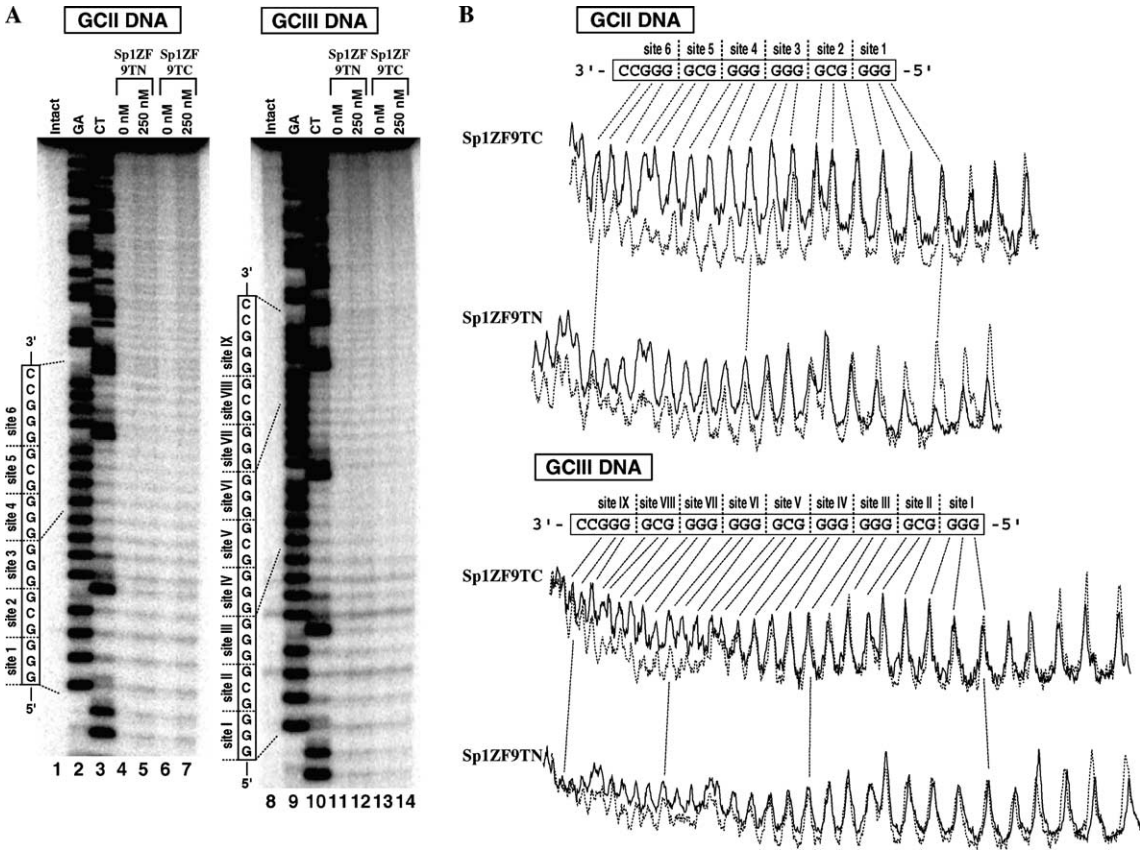

Fig. 5. Hydroxyl radical footprinting analyses for Sp1ZF9TC and Sp1ZF9TN bindings to GCII and GCIII DNAs. (A) Electrophoretic results of hydroxyl radical footprinting analyses. The left (lanes 1–7) and right (lanes 8–14) panels show the results for G-strand of GCII DNA and GCIII DNA, respectively. Lanes 1 and 8, intact DNA; lanes 2 and 9, G + A (Maxam–Gilbert reaction products); lanes 3 and 10, C + T (Maxam–Gilbert reaction products); lanes 4, 5, 11, and 12, Sp1ZF9TN; and lanes 6, 7, 13, and 14, Sp1ZF9TC. Protein concentrations are noted in the figures. (B) Densitometric analyses of the electrophoretic results. Solid and dotted lanes denote the cleavage intensities in the absence and presence of the protein, respectively.

proteins are the same. The guanine bases which are situated in the opposite strand of C-14, -19, and -20 in GCII DNA and C-22, -28, and -29 in GCIII DNA are recognized by both of the nine-zinc finger proteins, respectively. The X-ray crystallographic analyses of certain zinc finger–DNA complexes revealed that the zinc finger binds to DNA in a monomeric and anti-parallel binding mode and also recognizes a three-base-pair subsite by the one finger module [1,4]. In general, the four zinc finger domains should recognize specifically 12-bp-long DNA sequences. However, the results of methylation interference analyses show that G-12 and -13 in site 3 of GCII DNA and G-21 and -22 in site VI of GCIII DNA are not recognized in the bindings of the present two proteins. This result corresponds to the fact that, among the four successive zinc finger proteins, only the terminal zinc finger domain evidently makes a weaker contact with the guanine base [25]. Fig. 5A shows the footprinting patterns of the hydroxyl radical digestion on the substrate DNA for the bindings of the two proteins. The patterns of the DNA digestion between these two proteins were not substantially different (Fig. 5B). In the bindings of both proteins, the DNA sequences at sites 3–6 for GCII DNA and at sites VI–IX for GCIII DNA are fully protected from hydroxyl radical digestion by the protein bindings.

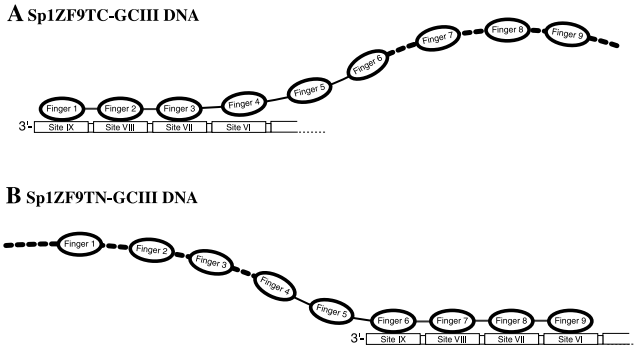

Fig. 6. Schematic representations of Sp1ZF9TN and Sp1ZF9TC bindings to GCIII DNA; (A) Sp1ZF9TC–GCIII DNA complex and (B) Sp1ZF9TN–GCIII DNA complex. The solid and dotted thick lines represent canonical (*Krüppel-type*) and TFIIIA-type linker sequences. The boxed area represents the GCIII DNA sites that the nine-zinc fingers recognize.

Effect of position of TFIIIA-type linker on DNA binding

The native nine-zinc finger protein, TFIIIA, contains the unique linker sequences between fingers 3–4, 4–5, 5–6, and 6–7, respectively. Here, we rename these unique linker sequences as TFIIIA-type. These linker sequences play an important role in DNA and RNA bindings of TFIIIA zinc finger protein [26]. However, it is unclear whether the positions of the linker sequence in the nine-zinc finger proteins affect DNA binding or DNA recognition. The three-zinc finger proteins that contain TFIIIA-type linker sequences (–NIKICV–, –TQQLP–, –AG–, and –QDL–) do not bind to the GC box DNA (unpublished data). In the present nine-zinc finger proteins, the finger portions containing TFIIIA-type linker sequences do not participate in DNA bindings. The TFIIIA-type linker sequences may inhibit the DNA binding of the zinc-finger domain because of its hydrophobic property [16]. The recognized regions of the substrate DNA suggest that our nine-zinc fingers use only four zinc finger domains for the DNA binding. Presumably, the domains of zinc fingers 1–4 and 5–9 participate in the DNA bindings of Sp1ZF9TC and Sp1ZF9TN, respectively (Fig. 6). These zinc finger domains are situated at the site opposite to the domains containing TFIIIA-type linker sequences. In the multi-zinc finger proteins, the position of the introduced TFIIIA-type linker sequence has an important effect on their DNA base recognitions. As well as the kind of the linkers, such as (*Krüppel-type*) and TFIIIA-type, therefore, the position of the linker is also pivotal in the design of multi-zinc finger proteins.

References

[1] C.O. Pabo, E. Peisach, R.A. Grant, Design and selection of novel Cys_2His_2 zinc finger proteins, Annu. Rev. Biochem. 70 (2001) 313–380.

[2] J.E. Coleman, Zinc proteins: enzymes, storage proteins, transcription factors, and replication proteins, Annu. Rev. Biochem. 61 (1992) 897–946.

[3] Q. Liu, D.J. Segal, J.B. Ghiara, C.F. Barbas III, Design of polydactyl zinc-finger proteins for unique addressing within complex genomes, Proc. Natl. Acad. Sci. USA 94 (1997) 5525–5530.

[4] N.P. Pavletich, C.O. Pabo, Zinc finger-DNA recognition: crystal structure of a Zif268–DNA complex at 2.1 Å, Science 252 (1991) 809–817.

[5] M. Yokono, N. Saegusa, K. Matsushita, Y. Sugiura, Unique DNA binding mode of the N-terminal zinc finger of transcription factor Sp1, Biochemistry 37 (1998) 6824–6832.

[6] M. Nagaoka, Y. Shiraishi, Y. Uno, W. Nomura, Y. Sugiura, Interconversion between serine and aspartic acid in the α-helix of the N-terminal zinc finger of Sp1: implication for general recognition code and for design of novel zinc finger peptide recognition complementary strand, Biochemistry 41 (2002) 8819–8825.

[7] E.J. Reber, C.O. Pabo, Zinc finger phage: affinity selection of fingers with new DNA-binding specificities, Science 263 (1994) 671–673.

[8] Y. Choo, A. Klug, Toward a code for the interactions of zinc fingers with DNA: selection of randomized fingers displayed on phage, Proc. Natl. Acad. Sci. USA 91 (1994) 11163–11167.

[9] Y. Choo, A. Klug, Selection of DNA binding sites for zinc fingers using rationally randomized DNA reveals coded interactions, Proc. Natl. Acad. Sci. USA 91 (1994) 11168–11172.

[10] M. Elrod-Erickson, C.O. Pabo, Binding studies with mutants of Zif268. Contribution of individual side chains to binding affinity and specificity in the Zif268 zinc finger–DNA complex, J. Biol. Chem. 274 (1999) 19281–19285.

[11] D.J. Segal, C.F. Barbas III, Design of novel sequence-specific DNA-binding proteins, Curr. Opin. Chem. Biol. 4 (2000) 34–39.

[12] N.P. Pavletich, C.O. Pabo, Crystal structure of a five-finger GLI–DNA complex: new perspectives on zinc fingers, Science 261 (1993) 1701–1707.

[13] J.H. Laity, J. Chung, H.J. Dyson, P.E. Wright, Alternative splicing of Wilms' tumor suppressor protein modulates DNA binding activity through isoform-specific DNA-induced conformational changes, Biochemistry 39 (2000) 5341–5348.

[14] K.R. Clemens, X. Liao, V. Wolf, P.E. Wright, J.M. Gottesfeld, Definition of the binding sites of individual zinc fingers in the transcription factor IIIA-5S RNA gene complex, Proc. Natl. Acad. Sci. USA 89 (1992) 10822–10826.

[15] X.B. Liao, K.R. Clemens, L. Tennant, P.E. Wright, J.M. Gottesfeld, Specific interaction of the first three zinc fingers of TFIIIA with the internal control region of the *Xenopus* 5S RNA gene, J. Mol. Biol. 223 (1992) 857–871.

[16] R.T. Nolte, R.M. Conlin, S.C. Harrison, R.S. Brown, Differing roles for zinc fingers in DNA recognition: structure of a six-finger transcription factor IIIA complex, Proc. Natl. Acad. Sci. USA 95 (1998) 2943–2983.

[17] T. Kamiuchi, E. Abe, M. Imanishi, T. Kaji, M. Nagaoka, Y. Sugiura, Artificial nine zinc-finger peptide with 30-base pair binding sites, Biochemistry 37 (1998) 13827–13834.

[18] M. Nagaoka, W. Nomura, Y. Shiraishi, Y. Sugiura, Significant effect of linker sequence on DNA recognition by multi-zinc finger protein, Biochem. Biophys. Res. Commun. 282 (2001) 1001–1007.

[19] M. Moore, Y. Choo, A. Klug, Design of polyzinc finger peptides with structured linkers, Proc. Natl. Acad. Sci. USA 98 (2001) 1432–1436.

[20] M. Moore, A. Klug, Y. Choo, Improved DNA binding specificity from polyzinc finger peptides by using strings of two-finger units, Proc. Natl. Acad. Sci. USA 98 (2001) 1437–1441.

[21] J.S. Kim, C.O. Pabo, Getting handhold on DNA: design of polyzinc finger proteins with femtomolar dissociation contacts, Proc. Natl. Acad. Sci. USA 95 (1998) 2812–2817.

[22] M. Brenowitz, D.F. Senear, M.A. Shea, G.K. Ackers, Quantitative DNase footprint titration: a method for studying protein, Methods Enzymol. 130 (1986) 132–181.

[23] J. Kuwahara, A. Yonezawa, M. Futamura, Y. Sugiura, Binding of transcription factor Sp1 to GC box DNA revealed by footprinting analysis: different contact of three zinc fingers and sequence recognition mode, Biochemistry 32 (1993) 5994–6001.

[24] T.D. Tullius, B.A. Dombroski, M.E.A. Churchill, L. Kam, Hydroxyl radical footprinting: a high-resolution method for mapping protein–DNA contacts, Methods Enzymol. 155 (1987) 537–558.

[25] M. Nagaoka, T. Kaji, M. Imanishi, Y. Hori, W. Nomura, Y. Sugiura, Multiconnection of identical zinc finger: implication of DNA binding affinity and unit modulation of the three zinc finger domain, Biochemistry 40 (2001) 2932–2941.

[26] R.F. Ryan, M.K. Darby, The role of zinc finger linkers in p43 and TFIIIA binding to 5S rRNA and DNA, Nucleic Acids Res. 26 (1998) 703–709.